

Linking Radar Data to Physical Models

A Major Qualifying Project Report

Submitted to the Faculty of the

WORCESTER POLYTECHNIC INSTITUTE

In partial fulfillment of the requirements for the

Degree of Bachelor of Science by

**Charles
Fancher**

**Glenn
Amundsen**

**Long
Tong**

**Genevieve
Boman**

Date: 15 October 2009

Sponsor: MIT Lincoln Laboratory, Supervisor: Dr. Stephen Weiner

WPI Advisor: Professor Germano Iannacchione

"This work is sponsored by the Missile Defense Agency under Air Force Contract #FA8721-05-C-0002. Opinions, interpretations, conclusions and recommendations are those of the author and are not necessarily endorsed by the United States Government"

Authorship

1 Introduction

1.1 Problem Statement and Motivation (CF, GA, LT)

1.2 Background

- . 1.2.1 History of Radar (GB)
- . 1.2.2 Overview of Radar Systems (LT)
- . 1.2.3 Space Vehicle Dynamics (GA)
- . 1.2.4 Scattering Centers (CF)
- . 1.2.5 Augmented Point Scatterer Model (GA)
- . 1.2.6 Range Time Intensity Plots (CF)
- . 1.2.7 Doppler Time Intensity Plots (CF)
- . 1.2.8 Radio Frequency Signature Toolbox (CF)

1.3 Plan for Tackling Problem

2 Methodology

2.1 Create Physical Models

- . 2.1.1 Offset Rocket (LT)
- . 2.1.2 Separating Rocket (GA)

2.2 Transforming physical models into Radar Data

- . 2.2.1 DAT File Creation (LT)
- . 2.2.2 Transforming Dat Files to Radar Data (CF)

2.3 Data Analysis

- . 2.3.1 Offset Rocket (CF)
- . 2.3.2 Separating rocket (GA GB)

3 Results/Discussion (CF GA GB LT)

4 Conclusions (CF GA GB LT)

Works Cited

**SIGNIFICANT PORTIONS OF THIS PROJECT WORK HAVE BEEN REPORTED IN AN
INTERNAL LABORATORY REPORT. MOST OF THAT TEXT WILL NOT BE REPEATED
HEREIN.**

Abstract

In outer space, the motion of targets is governed by Newton's laws of motion in three dimensions subject only to the force of rocket thrust. Radars can only make accurate measurements in one dimension as range (and range rate). The inability of radar systems to accurately obtain data beyond range measurements stimulated our research into the practical uses of radar data through the analysis of two scenarios: a rocket with an offset thrust and a tumbling two-part rocket separated by an offset impulse. The parameter space for both rocket scenarios was explored which resulted in relationships being observed between changing physical parameters and generated radar data. In certain cases, individual parameters were also found to have been quantifiable.

Executive Summary

Radar systems are great at detecting the range of objects in flight. However, there are limits on what other information they can ascertain. These limitations are the motivation for our project, which is focused on researching what useful information can be obtained from data retrieved from radar systems. There are many instances in which there is a need to know more about a given situation than just the range of an object.

The general plan for accomplishing this objective was to explore parameter space and try to link changes in parameter values with the effects they had on the trajectories and radar returns. The first task was to derive physical models for each situation so we could have a basis to generate the radar data from, and to which we could compare our results. From these equations of motion we determined parameters of interest which we thought would have an impact on the radar data. Once we derived these equations of motion and chose the parameters we wished to study we plotted the effects of varying these parameters on radar returns in the form of range time intensity (RTI) and Doppler time intensity (DTI) plots. Having the knowledge of what is going on physically and what the radar can see will let us compare them and link changes in physical parameters to changes in the radar data.

We were also able to calculate some relationships and specific parameters in both the offset thrust and separating scenarios from the radar data. For the offset rocket we were able to find a relationship between the steady state slope of the trajectory and the offset angle of the thrust. We were also able to determine that the angular velocity of the rocket was the only aspect of the trajectory that affected the RTI and DTI plots. In addition, we were able to determine which parameters changed the angular velocity. We learned that we could calculate the instantaneous velocity from DTI plots and use this as a piece of data to find a single parameter if we know all of the other parameters.

For the separating rocket we determined that, if we knew all other parameters, we could calculate the distance that the impulse was offset from the center of mass. For a rocket where less information was known, we could calculate many of the rocket's unknown parameters including the length of the objects in question, the magnitude of the angular velocities, and the angular orientation of the rocket at the separation. With some simplifying assumptions this can then be used to estimate the ratio of the changes in angular velocity for the two children and determine each of their shapes.

1 Introduction

1.1 Problem Statement and Motivation

Although radar systems are great at detecting the range of objects in flight, they have limits on what other information it can ascertain. It is because of these limitations that our project is focused on researching what useful information can be obtained from data retrieved from radar systems such as range time intensity (RTI) plots and Doppler time intensity (DTI) plots. There are many situations in which there exists a need to know more about a situation than the range of an object from a radar system.

For this project in particular, we will be looking at two situations. The first involves tracking the trajectory of a rocket which has its thrust at an angle offset from its center of mass. The second scenario involves looking at an already tumbling rocket that separates as a result of an impulse into its two constituent child components: a payload and a tank. In addition to the initial tumbling, the separating impulse may be offset from the center of mass which results in a change in angular velocity as well as linear velocity.

Previous work on this topic has been performed. In their 2006 Major Qualifying Project performed at MIT Lincoln Laboratory, Allen and Carveth discuss the observability of separation events using radar data. They looked at RTIs of separating rockets in an attempt to determine what parameters could be calculated from radar data. Although they started exploring the problem they were not able to reach any conclusions with in depth evidence (Allen & Carveth, 2006).

1.2 Background

1.2.1 History of Radar

Heinrich Hertz was the first to demonstrate the basic concept of radar. (History of Radar, 2005) He experimentally verified James Clerk Maxwell's theory of the electromagnetic field using an apparatus similar in principle to a pulse radar. He showed that radio waves could be reflected from metallic objects and refracted by dielectric prisms.

In the early 1900s Christian Hulsmeyer assembled a single pulse radar which was much improved over the apparatus used by Hertz. Hulsmeyer marketed his device for the detection of ships at sea in order to prevent collisions. However, there was not much interest in a collision-avoidance device. (Skolnik, 2001)

Other evidence of the radar method appeared in the 1920s. S.G. Marconi observed radio detection of targets in his experiments and urged its use in a 1922 speech delivered to the Institute of Radio Engineers. In 1922 A. Hoyt Taylor and Leo C. Young accidentally observed a fluctuating signal at their receiver when a ship passed between the receiver and transmitter, which were located on opposite sides of a river. Today, this is known as bistatic CW radar. Since the transmitter and receiver must be widely separated, this type of radar does not have significant utility. (Skolnik, 2001)

Military use of radar arose as a response to the heavy bomber aircraft of the late 1920s and early 1930s. Long range detection of an approaching bomber was important. In the 1930s, the radar method in which transmitter and receiver were located at a single site and pulsed waveforms were used, was developed independently by the United States, United Kingdom, Germany, Soviet Union, France, Italy, Japan, and the Netherlands. (Skolnik, 2001)

Early radars generally operated around 100-200 MHz, much lower than modern radars. The Chain Home radar system of Great Britain operated at 30 MHz, the low end

for pre-WWII, while the German Würzburg radars operated at the high end of the pre-war spectrum: 600 MHz. The technology utilized for radar was mostly an extension of then leading-edge radio communications technology. (Skolnik, 2001)

In 1940, the British invented the high-power microwave magnetron, enabling the use of higher frequencies for radar. In the fall of 1940 the British disclosed the magnetron invention to the U.S. for further development. With the cavity magnetron providing the technological basis, microwave radar technology developed rapidly in the United Kingdom and at MIT Radiation Laboratory and Bell Telephone laboratories in the United States during WWII. The MIT Radiation Lab was created specifically for this purpose, (History of Radar, 2005) and developed more than 100 different radar systems for military applications. (Skolnik, 2001)

1.2.2 Overview of Radar Systems

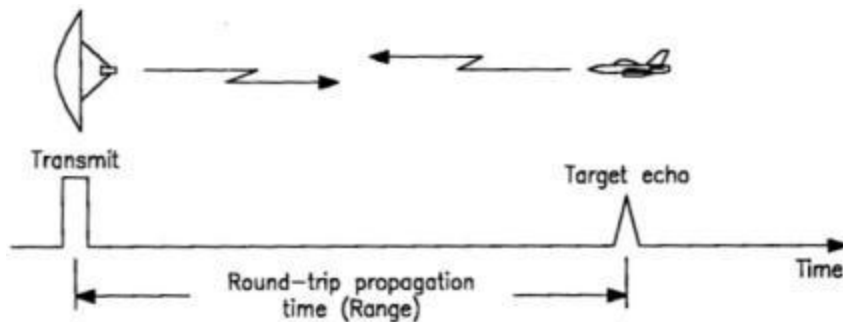


Figure 1-1: A radar antenna sends an electromagnetic pulse to a target which sends back an echo to the radar. (Edde, 1995)

RADAR is an acronym which stands for Radio Detection and Ranging. Radar systems help retrieve information about target positions in 3-d space as well as information about their velocities and orientation. The very basics of a radar system are illustrated by Figure 1-1. Here, a radio wave is first emitted from the radar antenna to the target. An echo is then sent back from the target to the radar antenna, due to back scatter. Certain information about the target can then be extracted based on the timing, power density, and other parameters of the echo signal received. Assuming for simplicity's sake that radio waves travel at the speed of light, c , in the atmosphere, the

round trip time it takes for a signal to be returned to the radar antenna from the time of transmission can be calculated as

$$\text{Round trip time} = \frac{2 \times \text{Range}}{c} \text{ [s]}.$$

Equation 1-1

Before we can go into some of the details of radar systems we first must define a coordinate system that can help explain some of the advantages and limitations of using radar systems. It's best to use spherical coordinates here as shown in Figure 1-2 since we will be discussing range (the 3-d distance from the radar, taken to be the origin, to the target) and angular position. The azimuthal angle is defined to be the beam angle position along the horizontal plane and the elevation angle to be the beam angle position along the vertical plane. (Edde, 1995)

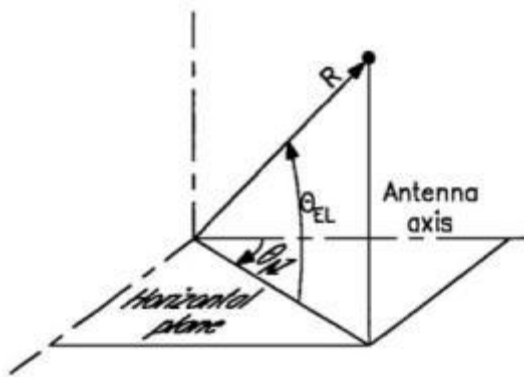


Figure 1-2: Coordinate system with the radar taken to be the origin. (Edde, 1995)

If we start out with a very basic radar antenna for a radar system we have what's called an isotropic antenna. That is, the power transmitted from the antenna is independent of angle and spreads out evenly over 3-d space. However, it is most often desirable to concentrate the transmitted power in a particular direction which can lead to greater range. To do this, the antenna's gain needs to be increased. Gain describes the ability to focus the radar beam in a given direction. Figure 1-3 illustrates the differences between a low gain antenna and a high gain antenna. (Edde, 1995)

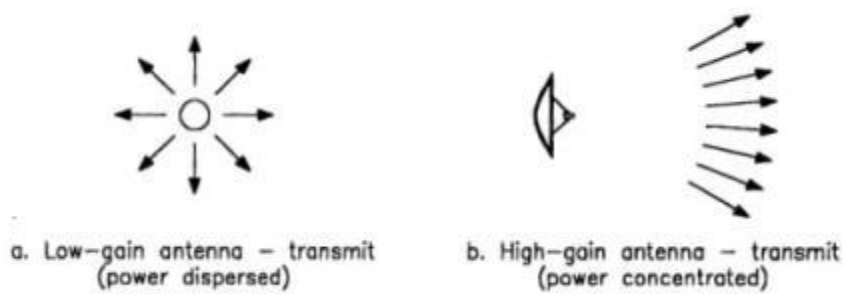


Figure 1-3: The larger the antenna gain, the more concentrated a radar's energy in one particular direction is. (Edde, 1995)

Another important parameter of radar systems is the angular resolution which is described by the radar's beam width in the azimuthal, $\Delta\phi$, and elevation directions, $\Delta\theta$.

$$\Delta\phi \sim \lambda/d \text{ [rad]}$$

Equation 1-2

$$\Delta\theta \sim \lambda/d \text{ [rad]}$$

Equation 1-3

d simply refers to the diameter of the antenna. Figure 1-4 gives a good illustration of beam width and why it is so important. The first antenna has a beam width so large that the radar is not able to resolve the two targets. The second radar has a much smaller beam width than the first antenna and thus has a greater angular resolution, which allows the radar the ability to recognize the two targets in space. (Edde, 1995)

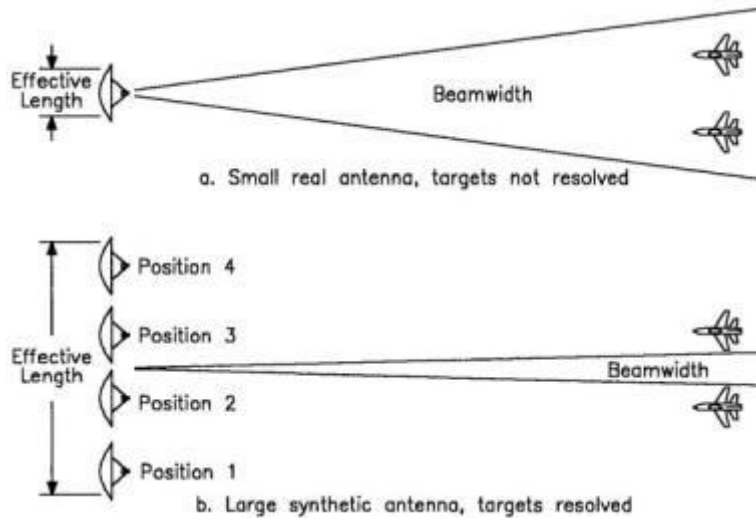


Figure 1-4: It's desirable to have as small a beam width as possible to help with resolution of targets. (Edde, 1995)

An important point to note here is that due to radio waves having much longer wavelengths than optical waves in the electromagnetic spectrum, their beam width is comparatively larger which results in their angular resolution to be low according to Equation 1-2 and Equation 1-3. The cross-range resolution, which is the ability of a radar system to separate targets at the same range, is also lowered dramatically due to low angular resolution. (Edde, 1995)

Another parameter of the radar system that is also affected by this lower angular resolution is the gain of an antenna. Taking into account inefficiencies such as losses due to heat dissipation, the gain of an antenna can be expressed in terms of the azimuthal and elevation beam width as

$$Gain = \frac{4\pi}{\Delta\theta\Delta\phi} [dimensionless].$$

Equation 1-4

Due to the increased beam widths along the azimuthal and elevation direction from using radio waves, the gain of an antenna is limited which further decreases the radar's ability to resolve targets. (Edde, 1995)

1.2.2.1 Radar Signature

All of the data collected from a particular target to the radar system is known as the target's radar signature. This information includes data about the radar cross section of the target and the target's Doppler spectrum. We explain in overview some of the components that make up the radar signature. (Cebula, Uftring, Whitmore, & Haddad, 2005)

1.2.2.2 Radar Cross Section

An important parameter to understand when analyzing the data collected from radar systems is the concept of the radar cross section (RCS), σ , of a target. The RCS simply describes how "big" the target appears to the radar and has units of $[m^2]$. It depends on the following three factors: the geometric cross section of the target, the reflectivity of the target, and the directivity of the backscattered beam from the target to the radar antenna. (Scott, 2004) (Adamy, 2004)

The geometric cross section refers to the cross sectional area of the target that actually intercepts the incident beam and is represented by $A [m^2]$. This depends primarily on the angle that the target makes with respect to the radar, also known as the aspect angle, with the zero angle referring to the nose of a target directly facing the radar antenna. Reflectivity refers to the fraction of the power scattered by the target to the power intercepted by the target and is defined as

$$Reflectivity = \frac{P_{scatter}}{P_{intercepted}} [dimensionless]$$

Equation 1-5

where $P_{intercepted} = A \times P_{incident}$. Directivity refers to the ratio of the power backscattered from the target that is actually directed back to the radar antenna to the power of the backscattered beam if it were to be radiated isotropically per unit solid angle,

$\left(\frac{1}{4\pi}\right)P_{scatter}$, and is defined as

$$\text{Directivity} = \frac{P_{backscatter}}{\left(\frac{1}{4\pi}\right)P_{scatter}} [rad].$$

Equation 1-6

Since the RCS is defined as the product of the geometric cross section, the reflectivity of the target, and the directivity of the backscattered beam, the RCS is given as

$$\sigma = (4\pi) \frac{P_{backscatter}}{P_{incident}} [m^2].$$

Equation 1-7

One really effective way of showing the RCS of a target is with a polar plot as shown in Figure 1-5. Here, a picture of the target is overlaid in the middle of the plot. The 2-d vector magnitude values here simply represent how large the RCS is from each angle of the target (in units of $[dBsm]$ instead of $[m^2]$) relative to the radar. The largest RCS values appear along the side of the target due to the large geometric cross section and the lowest values are around the corners and nicks around the plane. (Scott, 2004)

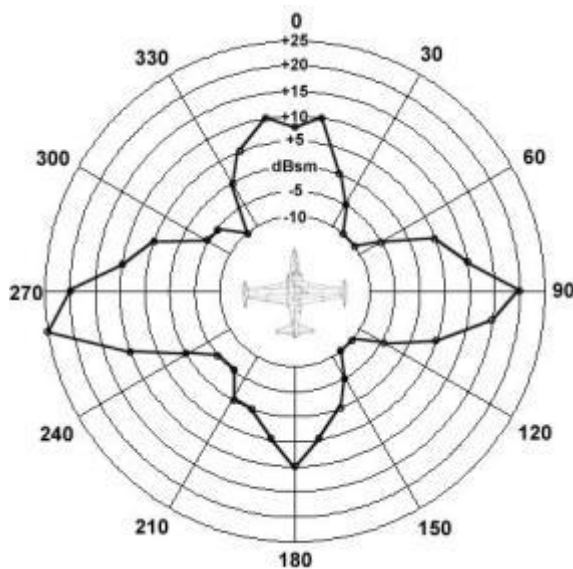


Figure 1-5: Radar cross section of two targets. (Scott, 2004)

Now that the radar cross section is defined, one last thing to look at is how the energy of the signal that is returned back to the radar antenna, S , after backscattering off of a target behaves as the range between the antenna and the target increases. The returned signal energy can be expressed in a proportionality relation as

$$S \propto \frac{\sigma}{R^4}$$

Equation 1-8

where R is the range between the target and the radar. The R^4 term comes from the fact that the transmitted radio wave signal is dissipating power over a region of the surface of a sphere roughly both ways (assuming the antenna has a relatively high gain). The significance of the return signal's energy dependence on the RCS can be quickly understood by Figure 1-6. As the range increases little by little, the energy of the signal coming back to the radar decreases rapidly. This means that the need to maximize the return energy signal by increasing the RCS as large as possible becomes even more important. (Scott, 2004)

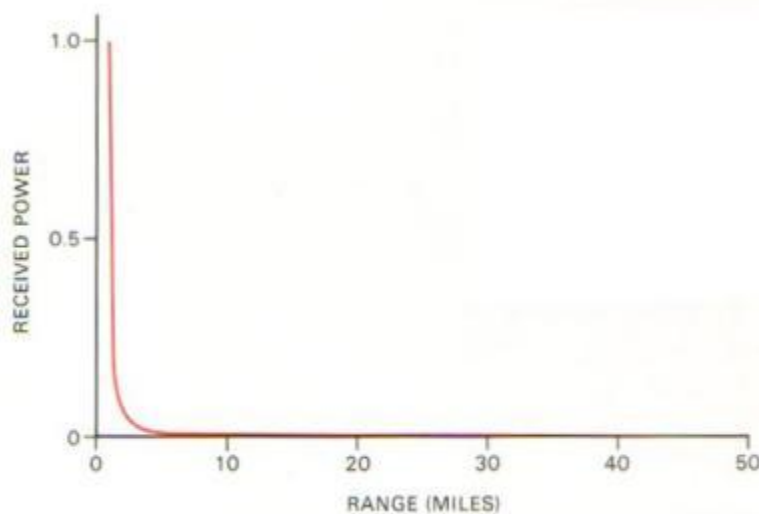


Figure 1-6: Plot of the return energy signal to the radar antenna versus the range between the antenna and the target. As you start increasing the range little by little, the return signal energy rapidly decreases. (Scott, 2004)

1.2.2.3 Doppler Spectrum

Another important component of the radar signature is the target Doppler spectrum. The Doppler spectrum is based on the Doppler shift which measures the change in frequency between two different waves. A Doppler shift is only measured when there exists moving targets with a radial velocity component. If the target is flying at a constant range with respect to the radar through time then no Doppler shift is recorded as shown in Figure 1-7.

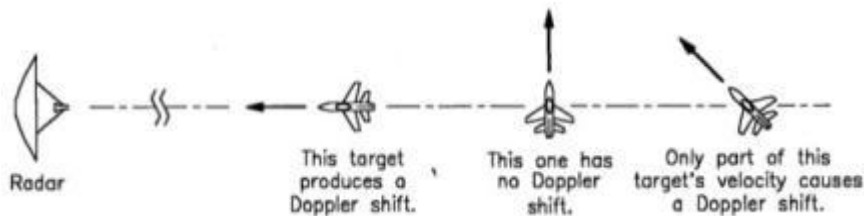


Figure 1-7: Targets that have a non-zero radial velocity register a Doppler shift. (Edde, 1995)

The Doppler shift, f_d , is defined as

$$f_d = f - f_0 \text{ [Hz]}$$

Equation 1-9

where f_0 is the frequency of the original transmitted signal and f is the frequency received at the observer. f is defined as

$$f = f_0 \left(\frac{v + v_R}{v + v_S} \right)$$

Equation 1-10

where v is the velocity of the signal relative to the medium, v_R is the velocity of the observer relative to the medium, and v_S is the velocity of the source relative to the medium. From Equation 1-9 and Equation 1-10, a positive Doppler shift occurs when the range between the radar and the target decreases (the target is approaching the radar

which results in a return frequency larger than the transmitted frequency) and a negative shift is recorded when the range increases between the radar and the target (the target is moving away from the radar which results in return frequency lower than the transmitted frequency). (Russell)

The Doppler spectrum comes into play when there are different parts of a target moving at different speeds relative to the radar. These differences in measured speed in turn gives different Doppler shifts which may be used to help identify the target's orientation and positioning. The relationship that describes the linear velocity at a point of a rotating object is given by

$$\vec{v} = \vec{r} \times \vec{\omega}$$

where r is the distance from the point to the object's center of mass and ω is the object's angular velocity.

One particular problem with the longer wavelength radio waves is that the Doppler shift measured is relatively small (due to the large wavelength) when transmitted signals scatter off of a target. This means that the time needed for the radar to be spent on the target must be greater in order to gather as many Doppler cycles as possible as the time needed to resolve the signals becomes greater. (Edde, 1995) (Kingsley & Quegan, 1999)

1.2.3 Space Vehicle Dynamics

There are many applications of rockets in space flight. Whether they are carrying a space shuttle, satellite, or nuclear warhead they must obey the basic laws of physics. Regardless of their purpose, most space vehicles have three main stages in their trajectory: Boost, Midcourse, and Re-entry (Weiner, 2004), see Figure 1-8.

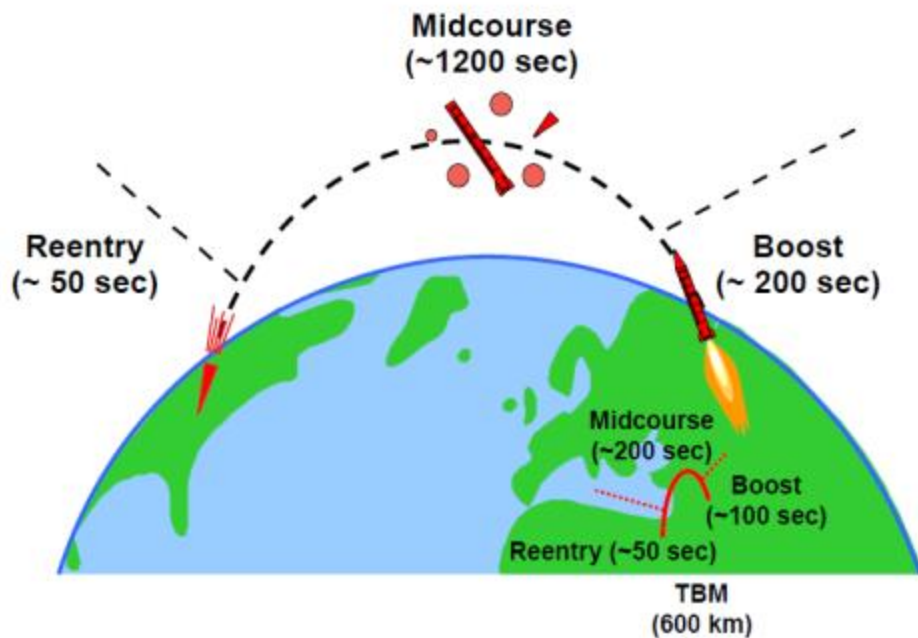


Figure 1-8: Rocket Trajectory

1.2.3.1 Boost Phase

The Boost Phase is the stage in which the rocket exits the Earth's atmosphere. The rocket's engines eject mass called "propellant" at very high speeds through its nozzles (Sellers, 1994). The force exerted on the propellant by the rocket causes the propellant to exert a force on the rocket due to Newton's third law: "every action has an equal and opposite reaction". The propellant is also exerting a force on the rocket. This process involves three main components. The first is "the combustion chamber" where the propellant is burned to produce hot gas. "The throat" controls the pressure in the combustion chamber and the flow rate of the gas. Finally the gas leaves through "the nozzle" which directs the expelled gas in the appropriate direction. (Sellers, 1994)

The magnitude of the force exerted by the ejected mass on the rocket is governed by conservation of momentum, which states that the total momentum of a system will remain constant in the absence of external forces. This implies that the change in momentum of the rocket must be equal to the change in momentum of the propellant being ejected. This change in momentum is simply the propellant's exhaust

velocity, V_{ex} , multiplied by the mass flow rate of the rocket, \dot{m} . This leaves us with Equation 1-11 (Taylor, 2005).

$$m\dot{v} = -m\dot{V}_{ex}$$

Equation 1-11

The right side of this equation is called the Thrust and can be understood as the cause of the force exerted on the rocket. Solving this equation by separation of variables and integrating gives Equation 1-12 (Taylor, 2005).

$$\Delta v = V_{ex} \ln \left(\frac{m_0}{m} \right)$$

Equation 1-12

This is the ideal rocket equation can be used to determine how much propellant is needed to obtain a certain change in velocity, Δv , with the difference between m_0 and m being the mass of the propellant (Sellers, 1994).

1.2.3.2 Midcourse Phase

The next phase of a rocket's trajectory is called Midcourse Phase. When the rocket runs out of fuel it is called "burnout". From there the objects follow a ballistic trajectory. Since the majority of this path takes place outside of the atmosphere, it can be assumed that air resistance is negligible, leaving only gravity to act on the rocket (Sellers, 1994).

The motion of the rocket is given by Equation 1-13 with R being the radial distance from the center of earth to the rocket, G being the Gravitational Constant, and M the mass of the earth. (Sellers, 1994)

$$\ddot{\hat{R}} + \frac{GM}{R^2} \hat{R} = 0$$

Equation 1-13

This equation, along with the velocity and position vectors at the time of burnout, defines the path that the rocket will take. What happens next depends on the original purpose of the rocket. When the payload separates from the booster it will either return to earth or continue on a trajectory through space.

1.2.3.3 Reentry Phase

The final phase of a rocket's trajectory occurs when the space vehicle returns to earth. During the Re-entry Phase, the payload travels through the atmosphere towards the earth's surface. Due to the object's large velocity you can assume that drag and lift are the dominant forces. When the object hits the atmosphere it is subject to immense drag, which causes massive deceleration of the payload. Energy lost from a space shuttle during Re-entry can reach 3.23×10^{12} Joules (Sellers, 1994). This energy is dissipated in the form of heat, which means that the vehicle re-entering the atmosphere must be able to withstand both large decelerations and high temperatures. Objects not designed to withstand these conditions, for example the boosters, will simply burn up during re-entry.

1.2.3.4 Scenarios of Interest

For this project we will be looking at two specific situations during space flight. The first scenario involves a rocket in the Boost Phase. This particular rocket has its nozzle at a slight offset so the thrust does not go straight through the body's center of mass. The result is that the thrust not only creates a linear force but also a torque on the rocket causing it to rotate.

The second scenario takes place in the Midcourse Phase. We will be looking at the separation of a rocket into its payload and boosters. In this example the rocket is initially tumbling and is then instantly separated by an impulse. However this impulse, similar to the thrust on the first rocket, is offset so it doesn't go through the center of mass. This means that not only will the impulse separate the two components of the rocket, but it will change their rates of rotation.

Space vehicles are complicated, dynamic systems, which can lead to many troubling situations. The rocket systems must be engineered perfectly to ensure success. And even then external factors such as weather and atmospheric conditions can affect the rocket's performance. (Chun, 2006) There is too much at stake in any space mission to leave anything up to chance, whether it's the extreme costs of a satellite, the human lives on a space shuttle, or the threat of a nuclear warhead in an Intercontinental Ballistic Missile (ICBM). That is why radar data of these space vehicles must be interpreted flawlessly to gather the most information possible about what is actually going on up there. This allows scientist and engineers to accurately test space systems, diagnose any problems that occur, and respond to any possible threats.

1.2.4 Scattering Centers

Scattering centers are places on radar targets from which the radar signal is returned. These centers are often places of discontinuity such as the nose of a cone or where the side of the cone meets the base. The two main categories of scatterers are point scatterers and specular scatterers. Point scatterers are so named because they represent a, more or less, point discontinuity that reflects waves back to the receiver. Specular scatterers are essentially the flat sides of objects. When these flat sides are perpendicular to the radar they return so much signal that it can be difficult for the radar to determine exactly where the scatterer is. The phenomenon that results from this is having sidelobes around the specular scatterer where the radar gives weaker returns across a wider range.

Not every part of a target will reflect enough of the signal back to the receiver to be detectable, leaving only small portions of each target that the radar can detect. Furthermore, each scatterer is not always visible. With rotating targets in particular, scattering centers are often shadowed by the rest of the target or by another target and go undetected because the radar waves cannot reach them.

1.2.5 Augmented Point Scatterer Model

The Augmented Point Scatterer Model (APSM) is a tool that is used to generate radar signatures. As discussed earlier, radar signatures contain all pertinent information about a target and APSM provides a convenient way to generate this information. Targets in APSM are defined by XML files, called configuration files, that include the coordinates of its center of mass and its various scattering centers. The scattering center's definition consists of a scattering type and strength, position relative to the center of mass, and the aspect angles for which it is in the radar's line of sight. (Cebula D., Uftring, Whitmore, & Haddad, 2005) These files are crucial for defining the radar signature of a target and will be used when generating simulated radar data.

1.2.6 Range Time Intensity Plots

The Range Time Intensity (RTI) plot is one of the traditional ways of displaying radar returns. The range relative to the center of mass is plotted on the x axis, time on

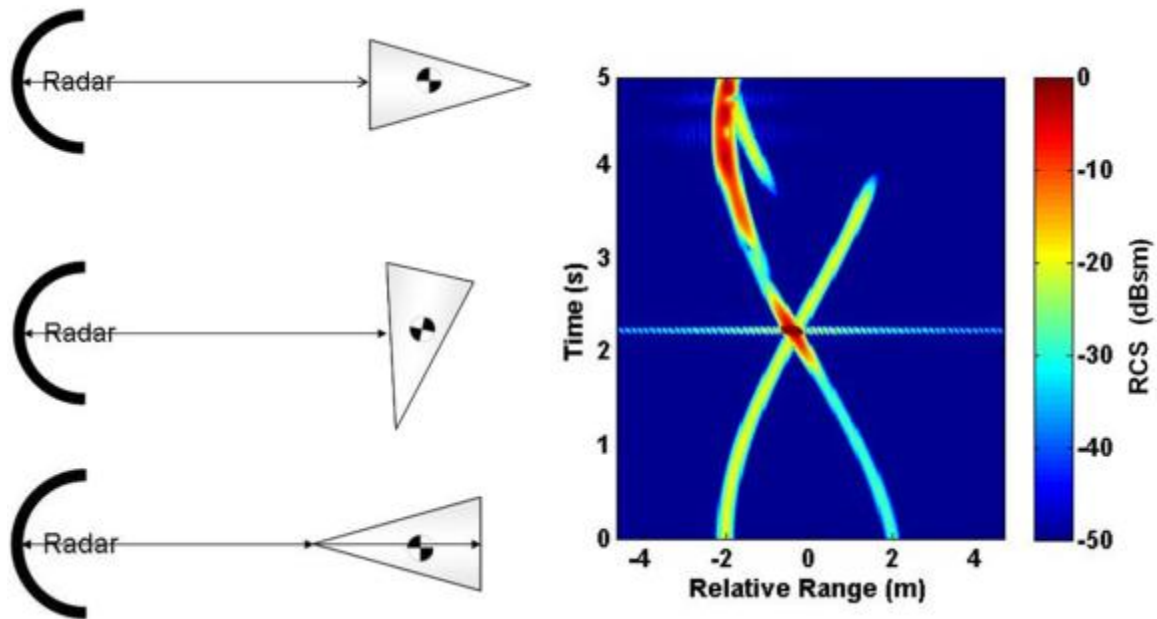


Figure 1-9: RTI plot and illustration (Martin, Static Pattern, 2009)

the y axis, and the intensity of the radar return on the color axis. The relative range is measured in the Radar Line of Sight (RLOS) axis, which points directly from the radar to the observed object where negative values are closer to the radar and positive values

farther away. These RTI plots are much different than a photograph of a situation and must be treated and analyzed much differently.

Figure 1-9 shows the simulated RTI plot of a tumbling cone. One of the scattering centers for a cone is at the nose, and the other two are where the sides meet the base. When the cone is facing the radar 'nose-on', as in the bottom left illustration, the radar waves are returned from the nose as well as the corners of the base of the cone. This corresponds to the RTI plot at $t = 0$ seconds where there are returns from the base at 2 meters and from the nose at -2 meters. As the cone rotates anti-clockwise the nose and back get closer to the center of mass in the RLOS frame. There are only two visible paths because one of the scatterers on the base of the cone is shadowed from the radar by the front of the cone.

The next interesting phenomena occurs just after $t = 2$ seconds and is shown in the middle left illustration. When the side of the cone is completely perpendicular to the RLOS there is a specular scatterer effect where the radar return is so strong that it is difficult for the radar to tell where exactly the signal is coming from. This results in the horizontal light blue band which is called a specular sidelobe.

After the cone has its side perpendicular it continues rotating with the nose getting farther away from the radar and the base getting closer. Just before $t = 4$ seconds the nose disappears and another track appears next to the base scatterer. This is due to the nose getting shadowed by the base of the cone and the second scatterer on the base of the cone coming into view of the radar.

The cone then continues to rotate until it has completed a 180 degree rotation by $t = 5$ seconds and the base is completely perpendicular to the RLOS. This causes both of the base scatterers to be the same distance away from the center of mass and results in their two tracks merging. We can note that, if the target were rotating clockwise, the RTI would look the same as in Fig 1-9. However, a DTI plot would look different.

1.2.7 Doppler Time Intensity Plots

Doppler Time Intensity (DTI) plots are quite similar to RTI plots with the difference being that they plot relative frequency against time instead of relative range against time. Shown below is the general Doppler shift formula for electromagnetic waves with f_0 being the initial frequency, c being the speed of light, v_r being the velocity of the receiver, v_s being the velocity of the source, and f_d is the Doppler shifted frequency.

$$f_d = \left(\frac{c + v_r}{c + v_s} \right) f_0$$

Equation 1-14: Doppler Shift Formula

In the case that a moving object reflects electromagnetic waves back to the source of the waves, we can manipulate the Doppler formula to find the velocity of the moving object, as seen below.

$$v = c \left(\frac{f_d - f_0}{f_d} \right)$$

Equation 1-15: Obtaining Velocity from Doppler Shift

Armed with the linear velocity of a scattering center it is possible to find its angular velocity if we know how far its distance from the center of mass, r .

$$\mathbf{v} = \mathbf{r} * \boldsymbol{\omega}$$

Equation 1-16: Linear Velocity

Figure 1-10 below shows the situation where the measured Doppler shift is zero. This is because the scattering centers at the nose and the base have all of their relative linear velocity oriented perpendicular to the RLOS. This creates zero net linear velocity in the RLOS frame, which leads to no Doppler shift.

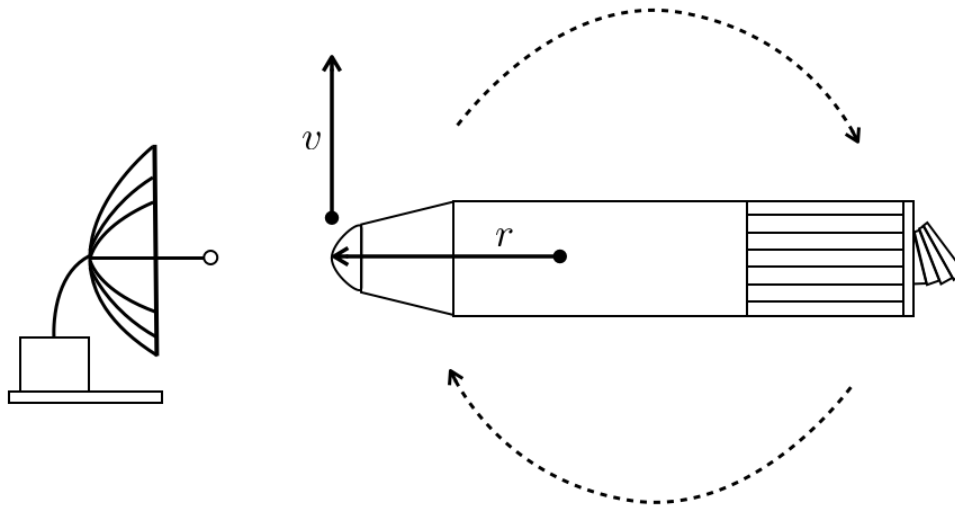


Figure 1-10: Diagram with Lowest Doppler Shift

Figure 1-11 shows when the Doppler shift would be highest because both the nose and back have all of their relative linear velocity parallel to the RLOS. This creates the highest possible v in the Doppler shift formula, which in turn creates the highest possible Doppler shift.

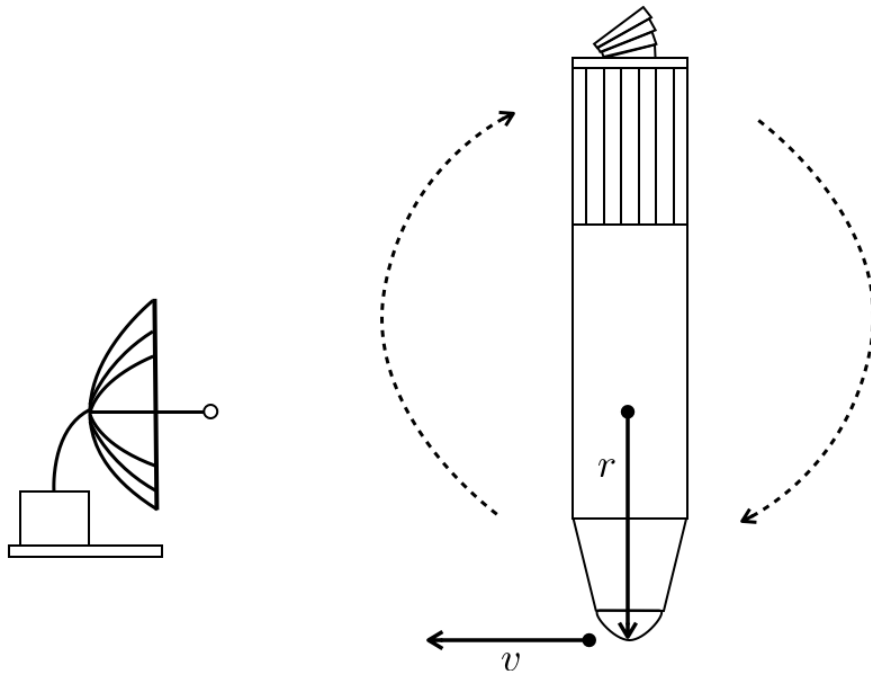


Figure 1-11: Diagram when Doppler Shift is Greatest

A sample DTI plot is shown in Figure 1-12. As you can see, with the cone oriented as in Figure 1-10 at $t = 0$ there is zero Doppler shift. With the cone oriented as in Figure 1-11 at $t = 2.3$, there is the highest Doppler shift.

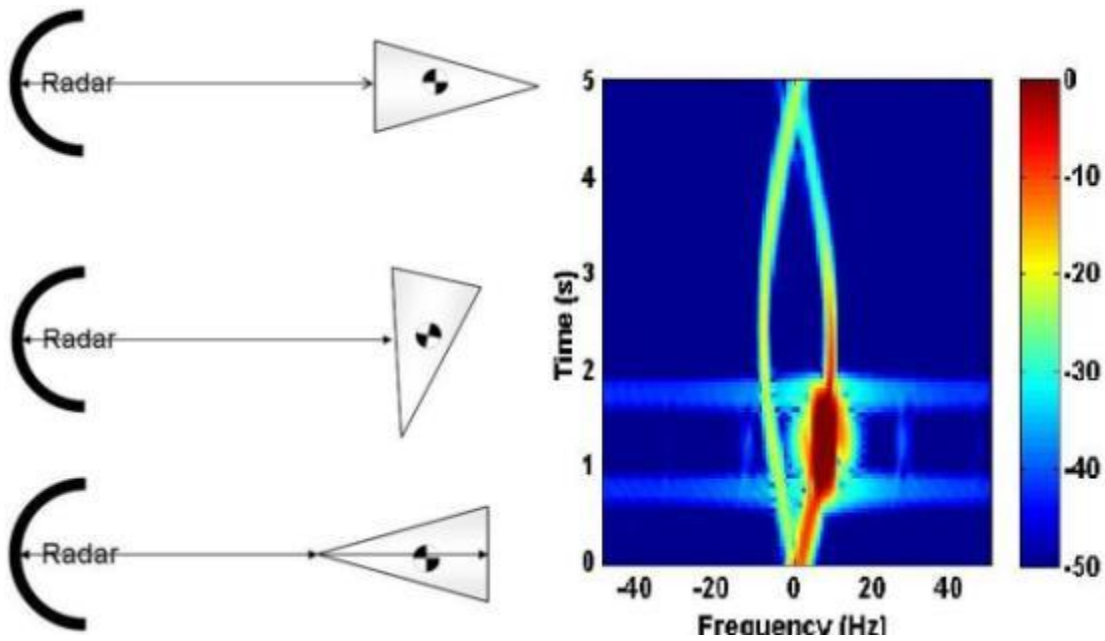


Figure 1-12: DTI plot of a tumbling cone

1.2.8 Radio Frequency Signature Toolbox

Radio Frequency Signature (RF Sig) is a software package that runs in MATLAB and is used for "... calculating radar returns from all objects in the complex using sensor parameters and producing range-time-intensity plots, Doppler-time-intensity plots, and range-Doppler images" (Carpenter & Cebula, 2005). RF Sig uses trajectory data from the standard output files to determine the location and orientation of each object, the sum total of all of the objects is called the complex, and combines that with APSM scatterer definition xml file for each object to create simulated radar returns. RF Sig can be used to create RTI, DTI and Range Doppler plots.

1.3 Plan for Tackling Problem

The general plan for tackling the problem of learning as much as possible from radar data is to explore the different parameters and try to link the changes to see what effect they have on the trajectories and radar returns. The first order of business is to derive the physical models for each situation so we can know what is going on. From these equations of motion we will determine parameters of interest to study that we think would have an impact on the radar returns. Once we have the equations of motion and the parameters we wish to study we will plot the effects of varying these parameters on radar returns derived from the equations we created. Having the knowledge of what is going on physically and what the radar can see will let us compare them and link changes in physical parameters to changes in the radar data.

2 Methodology

2.1 Create Physical Models

The first step of this project was to create physical models for the two scenarios that we are looking at. Using the laws of physics we had to solve for the equations of motion for both the offset rocket and the tumbling separating rocket. For both situations, we needed to first determine general specifications for a sample two part rocket. We looked up the mass and size of standard payloads and empty fuel tanks. From these sizes and masses we calculated the moment of inertia for both the offset rocket and the separating rocket.

To find the moment of inertia for the offset rocket about its center of mass, we employed the Parallel Axis Theorem which allows us to find the moment of inertia of an object in terms of the moment of inertia of its component objects. This is found by summing the individual moments of inertia for each component and also summing the products of each of the component masses with the square of the distance between the axis through each of the center of masses of each object parallel to the axis through the center of mass of the entire rocket.

Although the coordinate system will be discussed later on in the methodology of the report, the motion of the rocket in both scenarios will be restricted to the zx plane of the ENU coordinate frame.

2.1.1 Offset Rocket

In order to solve for the rocket's trajectory, the rocket's angular position as a function of time, $\phi(t)$ must be solved for. This can be accomplished by solving the analogue of Newton's Second Law for rotational bodies for torque as follows

$$\tau = I(t)\ddot{\phi}(t) = \vec{D} \times \vec{F}.$$

I is the (time dependent) moment of inertia of the rocket, D is the vector from the center of mass to the nozzle and F is the thrust vector. The z and x position of the offset rocket can be found as a function of time by solving Newton's Second Law

$$M(t)\vec{a}(t) = \vec{F}$$

in both the z and x directions

$$M(t)\ddot{z}(t) = F \cos(\phi(t) - \alpha)$$

$$M(t)\ddot{x}(t) = F \sin(\phi(t) - \alpha).$$

where $\phi(t)$ is the orientation of the rocket relative to the z -axis and α is the offset angle of the rocket's nozzle from the main axis of its body.

2.1.2 Separating Rocket

To create a physical model of the separating rocket we assumed that the net force and torque on the rocket were zero. We then calculated equations for the position and orientation of the rocket before separation using Equations 2-1 and 2-2.

$$X(t) = X_o + Vt$$

Equation 2-1: X Position

$$\phi(t) = \phi_o + \omega t$$

Equation 2-2: Phi position

Next, we calculated the trajectories of the fuel tank and payload after separation. We assumed that they were separated by an impulse that acted as an instantaneous change in momentum and angular momentum governed by Equations 2-3 and 2-4.

$$IM = m\Delta V$$

Equation 2-3: Effect of Impulse on linear velocity

$$x * IM = I \Delta\omega$$

Equation 2-4: Effect of Impulse on Angular velocity

The variable x is the distance that the impulse is offset from the center of mass and I is the moment of inertia. Using these equations and conservation of momentum we were able to calculate the velocities and angular velocities of both the tank and the payload. From there we used equations 2-1 and 2-2 again to calculate the trajectories.

Another issue that needs to be addressed when developing a physical model for the separating rocket is determining if the two components are going to collide after separation. Any collision would affect the trajectories and need to be taken into account. We created a Matlab script that modeled the motion of the center of masses of each object and then expanded that to model the trajectory of each of the corners as the object tumbled through space. Next, we added code to see if any of the corners of one object crossed between a line connecting two corners of the other object. Finally, we animated this to visually verify that our script accurately tested for collisions.

2.2 Transforming physical models into Radar Data

2.2.1 DAT File Creation

In order to generate radar plots based on a rocket's trajectory which include RTI and DTI plots, we must first create a DAT file specific to each particular rocket trajectory. DAT files are 22 column ASCII files which contain all of the necessary information about an object to create simulated radar plots during its flight. The 22 pieces of information about the object include the following:

1. *Time*
2. *x (ECI)*
3. *y (ECI)*
4. *z (ECI)*
5. *v_x (ECI)*
6. *v_y (ECI)*
7. *v_z (ECI)*
8. *w_x*
9. *w_y*
10. *w_z*
11. *x-body-x*
12. *x-body-y*
13. *x-body-z*
14. *y-body-x*
15. *y-body-y*
16. *y-body-z*
17. *z-body-x*
18. *z-body-y*
19. *z-body-z*
20. *Latitude [deg]*
21. *Longitude [deg]*
22. *Altitude [km]*

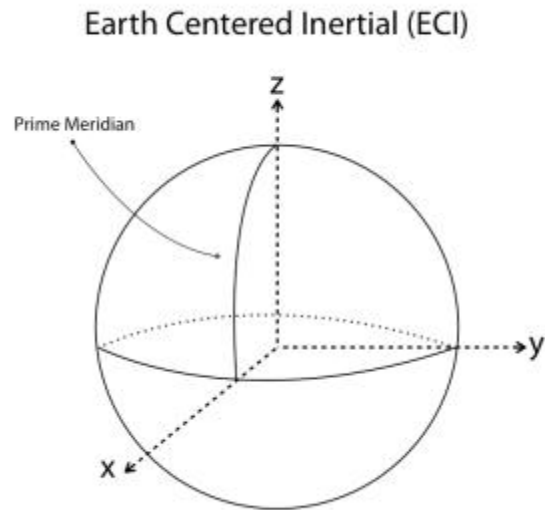


Figure 2-1: The ECI coordinate system at time

Before we begin to explain what each of the individual columns are, we first must mention the coordinate systems that will be used when creating our physical models. The first one is the Earth Centered Inertial (ECI) coordinate system as shown in Figure 2-1. In this coordinate system the origin is located at the center of the Earth, with the x-axis pointing towards the Prime Meridian and 0° latitude, the y-axis pointing towards 90° East and 0° latitude, and the z-axis pointing towards the North Pole orthogonal to both the x-axis and y-axis at time $t = 0$ [s]. Here, time is measured relative to the Greenwich Mean Time (GMT) time zone. To make our physical model simple, we'll position our rocket such that its motion will only be in the GMT time zone within the period of time that we run our simulation. The time passed during the rocket's flight from the initial time $t = 0$ to some future time t is what constitutes the data in column 1 in the DAT file.

Using ECI coordinates is important mainly due to the fact that DAT files require the parameters of an object's trajectory in ECI coordinates for its position and velocity vectors. It's also important due to the fact that it's an inertial coordinate frame meaning that its axes stay fixed in space with increasing time (even as the Earth rotates). This

makes it easy to use without having to deal with as many coordinate transformations as required by using other coordinate systems.

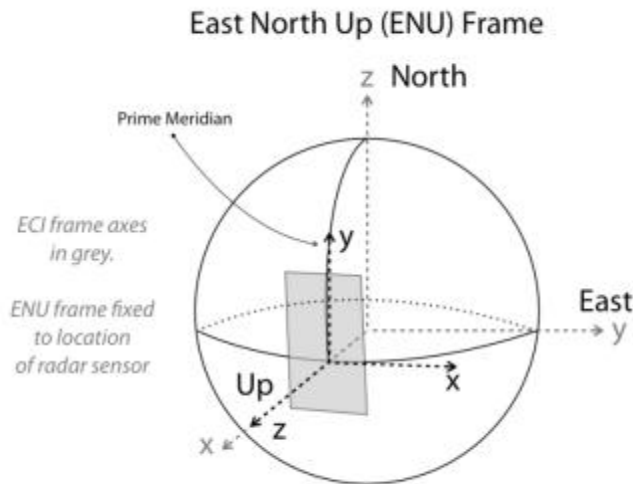


Figure 2-2: The ENU coordinate system at time $t = 0$ [s].

One other coordinate system that is being used for our project is called the East, North, Up (ENU) coordinate system as shown in Figure 2-2 where it is overlaid on the ECI coordinate system at time $t = 0$ [s]. Here, the origin of the coordinate frame is actually fixed on the location of the radar sensor itself. By default, the radar sensor will be placed on the surface of the Earth at the intersection of the Prime Meridian and the equator giving it a coordinate of $(0^\circ, 0^\circ, 0 \text{ [km]})$. The grey plane shows that the coordinate system is tangential to the surface of the Earth at that point. The x-axis is defined to be pointing towards East, the y-axis as pointing towards North, and the z-axis as pointing up (or perpendicular to the surface of the Earth).

Using ENU coordinates is useful because measurements made on the Earth are made in ENU coordinate space which means that they don't need to be transformed when working only in the ENU Frame. However, coordinate transformation from ENU to ECI is necessary for the creation of the DAT files and is accomplished easily by calling a coordinate transformation Java method from the MIT Lincoln Laboratory BMD Toolbox. From this point on, assume all motion of the rocket to be in reference to the ENU

coordinate frame unless explicitly stated otherwise.

Columns 2-4 of the DAT file simply specify the rocket's Cartesian coordinates in 3-d space in ECI coordinates. To simplify things at the current time, we'll restrict the rocket's trajectory and its tumbling to the xz plane only in ENU coordinates which means the y component of the rocket will always be 0 (in ECI, this corresponds to the z component being with the rocket traveling in the xy plane). The z and x position of the rocket can be found as a function of time by solving Newton's Second Law

$$M(t)\vec{a}(t) = \vec{F}$$

in both directions

$$M(t)\ddot{z}(t) = F \cos(\phi(t) - \alpha)$$

$$M(t)\ddot{x}(t) = F \sin(\phi(t) - \alpha).$$

where $\phi(t)$ is the orientation of the rocket relative to the z -axis and α is the offset angle of the rocket's nozzle, respectively. One note to mention here is that we must be sure to give the rocket an initial position such that the rocket will not travel below the surface of the Earth in order to make the simulation match physical reality as close as possible.

Columns 5-7 refer to the rocket's velocity in the x , y and z direction in ECI coordinates. In the process of solving for the rocket's position as a function of time by using Newton's Second Law, the velocity of the rocket is easily found along the z and x directions in the ENU frame (and in the x and y directions in the ECI frame by using the coordinate transformation Java method). And similar to the reasoning for the y component of the position of the rocket being equal to 0, the velocity along the y direction will also be 0 here as well.

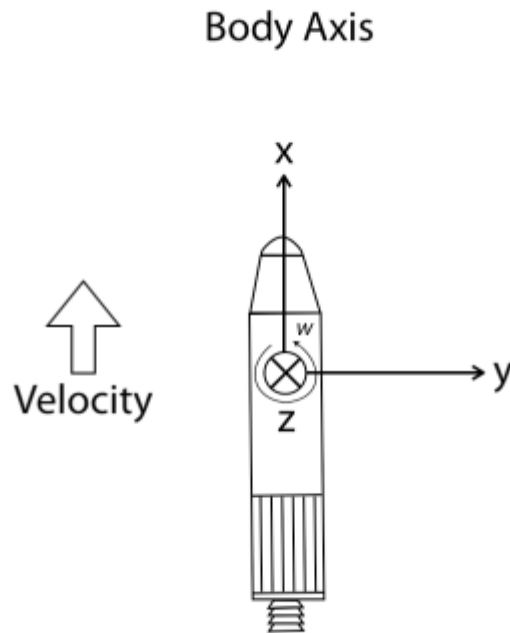


Figure 2-3: The rocket's own internal body axis.

Columns 8-10 refer to the rocket's angular velocity with respect to its own body axis. Figure 2-3 shows how the axis of the rocket's own internal coordinate system is oriented relative to its direction of propagation. It is convention for the x-axis to be pointed along the direction of the object's propagation, the y-axis pointed along the right wing of the object and orthogonal to the x-axis, and the z-axis pointed downward and orthogonal to all of the other axes. Figure 2-4 shows how the rocket is oriented relative to the ENU coordinate system. Using the fact that we are restricting the rocket to travel only in the zx plane, this means that the angular velocity of the rocket is 0 about both the x and y axes. The angular velocity of the rocket about the z-axis can be found by solving the analogue of Newton's Second Law for rotational bodies as follows

$$\tau = I(t)\ddot{\phi}(t) = \vec{D} \times \vec{F}$$

$$I(t)\ddot{\phi}(t) = DF \sin(\alpha.)$$

Top-down View

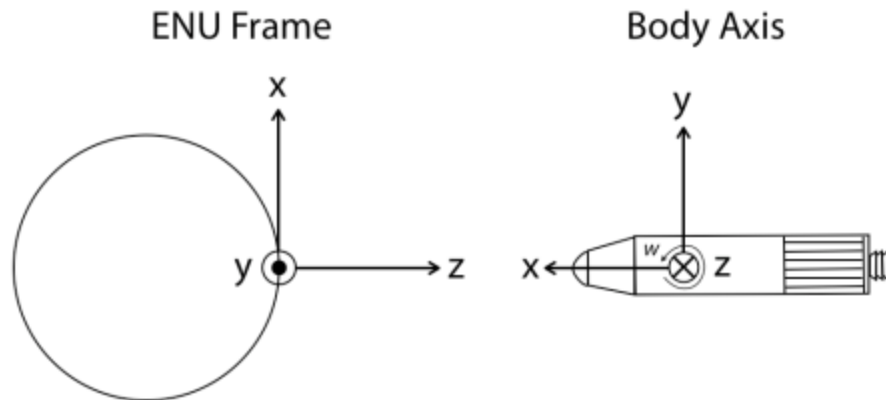


Figure 2-4: Orientation of the rocket relative to the ENU coordinate system.

Columns 11-19 are values that relate how the rocket's own internal coordinate system is oriented relative to the ENU coordinate system (or any other coordinate system for that matter). In fact, they're simply elements of what's known as the direction cosine matrix (sometimes abbreviated as DCM). The direction cosine matrix, A , is defined as the product of individual matrices as

$$A = [A_x][A_y][A_z]$$

where A_x , A_y and A_z are the matrices for rotations only about the x, y and z-axes, respectively. They are each defined as

$$A_x = \begin{bmatrix} 1 & 0 & 0 \\ 0 & \cos(\phi) & \sin(\phi) \\ 0 & -\sin(\phi) & \cos(\phi) \end{bmatrix}$$

$$A_y = \begin{bmatrix} \cos(\theta) & 0 & -\sin(\theta) \\ 0 & 1 & 0 \\ \sin(\theta) & 0 & \cos(\theta) \end{bmatrix}$$

$$A_z = \begin{bmatrix} \cos(\psi) & \sin(\psi) & 0 \\ -\sin(\psi) & \cos(\psi) & 0 \\ 0 & 0 & 1 \end{bmatrix}$$

with ϕ , θ and ψ being the angular displacement about the x, y and z-axis following convention, respectively. Since the rocket is restricted to motion in only the zx plane in ENU coordinates, the only angular displacement we need to be concerned about is rotation about the rocket's z body axis since the rotations about the x and y axis are zero and, as a result, reduces matrices A_x and A_y both down to the identity matrices. This leaves us with only the z component of the direction cosine matrix as the value of the direction cosine matrix itself as follows

$$A = [A_x][A_y][A_z]$$

$$A = [I][I][A_z]$$

$$A = [A_z].$$

From here on out, we will use $\phi(t)$ to represent the angular position of the object rather than $\psi(t)$ to reduce the amount of different symbols used.

Column 20 refers to the latitudinal coordinate of the rocket at time t . Exploiting the fact that we are restricting the rocket's motion to only the plane again, this means that the rocket's latitudinal position is always going to be 0° for all time t .

ENU Top-down View

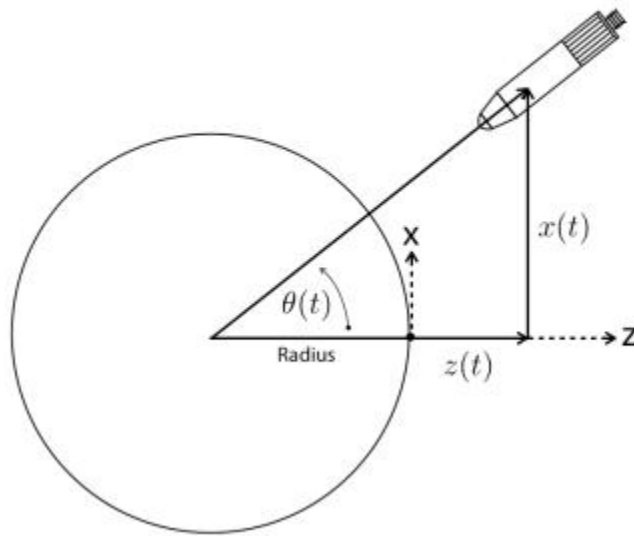


Figure 2-6: The longitudinal position of an object is easily computed using simple trigonometry.

$$Longitude(t) = \arctan\left(\frac{x(t)}{Radius + z(t)}\right) \left(\frac{180}{\pi}\right) [\text{deg}]$$

where the factor $\left(\frac{180}{\pi}\right)$ is used for converting the angle from $[rad]$ to $[deg]$.

2.2.2 Transforming Dat Files to Radar Data

Once the trajectory information is stored in dat files, there are still more steps that need to be taken to create simulated radar returns for analysis. In one of the oddities of programming, after all of the trajectory data is written to the dat files it has to be read back into memory. Each entity in the simulation (unitary rocket, tank, Payload, etc.) has its own trajectory dat file which gets input into a separate java trajectory object in memory. This is necessary for the Matlab script to interpret the data correctly.

The next step is to create a time history java object for each entity. This is accomplished by using a java method which combines sensor data defined in the variable initialization script `testsim.m` with each trajectory object to create a unique time history object for each entity. What this essentially does is convert the trajectory information from coordinates that are relative to the earth (the ECI X,Y,Z positions and velocities, and latitude, longitude, altitude) and the internal coordinate frame (direction cosine matrix and rotation rates) into information that is all relative to the sensor. The 22-columns of trajectory information are converted into 11- columns that are: Time, Azimuth, Elevation, Range, Aspect, Roll, Orientation, Offset, NoiseFloor, PulseNumber, and Center Freq.

It is at this point that radar imperfection like range limits, horizon limits, angular uncertainties, and many other aspects of realistic radars can be added. For our project we ignored these aspects for the most part. We determined that things like being able to look over the horizon and having a low signal to noise ratio at long distances would allow us to focus more on the physics of the project and less on the technical details of radar systems.

The last step in converting all of the data is to create a java object called a track for each entity in the simulation. This is done by combining the time history information for each entity with the xml scattering definition file. What this does is attach the

“frame” of scattering centers to the point object that we have been working with until now. There is an important difference between the separating rocket situation and the offset rocket situation in this step. With the separating rocket, there is a cell array of tracks that gets created from the individual java objects, while in the offset rocket there is only one object to track.

Once there are ‘track’ java objects for each entity, we used the RF Sig software to generate simulated radar returns in the form of RTI and DTI plots. The RF Sig software takes the tracks and combines them with inputs that control how the returns are plotted like the maximum relative range in RTI plots or the timeframe to calculate the returns for. One input parameter that can have a large impact on what the plots look like is the centering track in the separating rocket situation. The centering track is the zero relative range that all of the other tracks are based off of. The effect this has is that if the other entities translate away from the centered track, then the relative ranges of their scattering centers are no longer relative to their individual centers of gravity, but to the center of gravity of the centered track.

2.3 Data Analysis

In order to begin our analysis we first needed to choose which physical parameter to explore for both the offset and separating rocket. We focused on the parameters that we thought would have an impact on the trajectory of the rocket and the radar data in the form of RTI and DTI plots. We also went over this set of parameters with our advisors to receive input and ratification on our choices.

2.3.1 Offset Rocket

Table 2-1 below shows the baseline parameters we chose and the minimum and maximum values we assigned them when varying them. These values were selected based on our knowledge of what would be possible for a rocket to have.

| Parameter | Baseline Value | Lowest Value | Highest Value |
|--------------------------|----------------|--------------|---------------|
| Offset Angle (rad) | $\pi / 18$ | 0 | $\pi / 2$ |
| Mass of Fuel (kg) | 10000 | 100 | 100000 |
| Mass of Payload (kg) | 1000 | 100 | 100000 |
| Burnout Time (s) | 60 | 15 | 240 |
| Exhaust Velocity | 600 | 10 | 5000 |
| k_inertia | 5 | .1 | 20 |
| Torque Arm (m) | 3.6 | .1 | 6 |
| Initial Z Velocity (m/s) | 0 | 0 | ?? |
| Initial X Velocity (m/s) | 0 | 0 | ?? |

Table 2-1: Table of Baseline, Minimum, and Maximum Values for Parameters

2.3.1.1 Steady State Trajectory

One of the aspects of the offset rocket that we were interested in investigating was where it would eventually end up going. To do this we plotted the trajectory of the

rocket with the baseline parameters and determined whether there was a way to define the trajectory after a long time or the steady state trajectory. We calculated a line of best fit and determined that its slope would be a good indication of the rocket's destination.

To see what effect different parameters had on the trajectory slope, we varied all of the parameters and plotted the resulting slopes against the baseline slope we calculated. The parameters we varied in this manner were the nozzle offset, mass of the payload, the exhaust velocity, the mass of the fuel, the burnout time, and the distance from the back of the rocket to the center of mass.

2.3.1.2 Radar Returns

In order to determine the effect of varying different parameters on radar returns, we varied the parameters of the offset rocket then looked at the effect created on the RTI and DTI plots. We also computed final angular velocities and the resulting final angular positions in order to get numerical results we could more easily analyze. We then determined what correlation there was, with any of the parameters varying the parameters of the offset rocket by comparing these final angular velocities and positions. The parameters we studied were the offset angle, the mass of the fuel, the mass of the payload, the initial velocity in the Z direction, the initial velocity in the X direction, the exhaust velocity, and the burnout time.

2.3.2 Separating rocket

One parameter was systematically varied using "For" loops in Matlab, while all other parameters were held constant. The resulting radar images were visually compared in order to determine if we could observe the differences predicted by the equations. After correcting errors found in the Matlab code, we were able to observe that variations of the independent variables affected the expected characteristics of the radar images.

We next wrote Matlab code that enabled us to quantify and record the RTI variations which we were observing. The data for each dependent variable was plotted vs. the independent variable in order to determine if any trends exist.

3 Results/Discussion

We were able to calculate some relationships and specific parameters in both the offset thrust and separating scenarios from the radar data. For the offset rocket we were able to find a relationship between the steady state slope of the trajectory and the offset angle of the thrust. We were also able to determine that the angular velocity of the rocket was the only aspect of the trajectory that affected the RTI and DTI plots. In addition, we were able to determine which parameters changed the angular velocity. We learned that we could calculate the instantaneous velocity from DTI plots and use this as a piece of data to find a single parameter if we know all of the other parameters.

For the separating rocket we determined that, if we knew all other parameters, we could calculate the distance that the impulse was offset from the center of mass. For a rocket where less information was known, we could calculate many of the rocket's unknown parameters including the length of the objects in question, the magnitude of the angular velocities, and the angular orientation of the rocket at the separation. With some simplifying assumptions this can then be used to estimate the ratio of the changes in angular velocity for the two children and determine each of their shapes.

Specific results and discussion of the results are documented in a separate internal Lincoln Laboratory report.

4 Conclusions

Radar systems are great at detecting the range of objects in flight. However, there are limits on what other information they can ascertain since they only measure range (and range rate) accurately. These limitations are the motivation for

our project, which is focused on researching what useful information can be obtained from data retrieved from radar systems for the physical scenarios considered. There are many instances in which there is a need to know more about a given situation than just the range of an object.

More detailed conclusions for the specific problems addressed are documented in a separate internal Lincoln Laboratory report.

Works Cited

- Adamy, D. (2004). *EW 102: A Second Course in Electronic Warfare*. ArTech House, Inc.
- Allen, B., & Carveth, C. (2006). *Observability of Separation Events Using Radar Data*. Worcester: Worcester Polytechnic Institute; MIT Lincoln Laboratory.
- Carpenter, M., & Cebula, D. P. (2005). *MATLAB Radar Scene Generation Toolbox*. Lexington: MIT Lincoln Laboratory.
- Cebula, D. P., Uftring, S., Whitmore, M., & Haddad, P. (2005). *Radar Signature Generation Using the Augmented Point Scatterer Model (APSM) v3.1*. Lexington: MIT Lincoln Laboratory.
- Chun, C. (2006). *Thunder Over the Horizon*. Westport: Praeger Security International.
- Edde, B. (1995). *Radar Principles, Technology, Applications*. Upper Saddle River: Prentice Hall, PTR.
- History of Radar*. (2005). Retrieved August 31, 2009, from Fact-Archive: http://www.fact-archive.com/encyclopedia/History_of_radar#Comparison
- Kingsley, S., & Quegan, S. (1999). *Understanding Radar Systems*. Mendham: SciTech Publishing, Inc.
- Martin, J. (2009, Aug 10). *LL6D*. Retrieved Aug 28, 2009, from Renegade Confluence: <http://renegade/confluence/display/RMW/LL6D>
- Martin, J. (2009, August 10). *Static Pattern*. Retrieved August 21, 2009, from Renegade Confluence: <http://renegade/confluence/display/RMW/Static+pattern>
- Russell, D. A. (n.d.). *The Doppler Effect and Sonic Booms*. Retrieved October 14, 2009,

from Kettering University:

<http://paws.kettering.edu/~drussell/Demos/doppler/doppler.html>

Scott, J. (2004, March 21). *Aerospaceweb.org | Ask Us - Radar Cross Section*. Retrieved September 3, 2009, from Aerospaceweb.org: Aerospaceweb.org | Ask Us - Radar Cross Section

Sellers, J. J. (1994). *Understanding Space: An Introduction to Astronautics*. New York: McGraw-Hill, Inc.

Skolnik, M. I. (2001). *Introduction to Radar Systems, Third Edition*. New York: McGraw-Hill.

Taylor, J. R. (2005). *Classical Mechanics*. Sausalito: University Science Books.

Weiner, S. (2004, February 24). BMD Systems Analysis Lecture. Lexington, MA, USA: Unpublished.